



저작자표시-비영리-변경금지 2.0 대한민국

이용자는 아래의 조건을 따르는 경우에 한하여 자유롭게

- 이 저작물을 복제, 배포, 전송, 전시, 공연 및 방송할 수 있습니다.

다음과 같은 조건을 따라야 합니다:



저작자표시. 귀하는 원저작자를 표시하여야 합니다.



비영리. 귀하는 이 저작물을 영리 목적으로 이용할 수 없습니다.



변경금지. 귀하는 이 저작물을 개작, 변형 또는 가공할 수 없습니다.

- 귀하는, 이 저작물의 재이용이나 배포의 경우, 이 저작물에 적용된 이용허락조건을 명확하게 나타내어야 합니다.
- 저작권자로부터 별도의 허가를 받으면 이러한 조건들은 적용되지 않습니다.

저작권법에 따른 이용자의 권리는 위의 내용에 의하여 영향을 받지 않습니다.

이것은 [이용허락규약\(Legal Code\)](#)을 이해하기 쉽게 요약한 것입니다.

[Disclaimer](#)

**Discovery of Biomarkers for
Predicting Aggressive Small Renal Cell Cancer**

Jongchan Kim

**The Graduate School
Yonsei University
Department of Medicine**

Discovery of Biomarkers for Predicting Aggressive Small Renal Cell Cancer

**A Dissertation Submitted
to the Department of Medicine
and the Graduate School of Yonsei University
in partial fulfillment of the
requirements for the degree of
Doctor of Philosophy in Medical Science**

Jongchan Kim

June 2024

**This certifies that the Dissertation
of Jongchan Kim is approved.**

Thesis Supervisor Won Sik Ham

Thesis Committee Member Woong Sub Koom

Thesis Committee Member Sang Joon Shin

Thesis Committee Member Jaemoon Yang

Thesis Committee Member Serk In Park

**The Graduate School
Yonsei University
June 2024**

ACKNOWLEDGEMENTS

First and foremost, I would like to express my gratitude to my advisor, Prof. Won Sik Ham. Prof. Ham has guided me since my residency and throughout my fellowship, despite my shortcomings. My current position at Yongin Severance Hospital and my pursuit of a Ph.D. are all thanks to him. His rational decision-making and never-ending pursuit of challenges in both clinical and research settings are truly admirable and something that I, as a junior and a disciple, aspire to emulate. I will continue to learn from you and remember to repay the kindness you have shown me.

I would also like to thank the committee members: Prof. Woong Sub Koom, Sang Joon Shin, Jaemoon Yang, and Serk In Park for their valuable advice, which encouraged me to delve deeper into my studies and helped me produce a better dissertation.

I am sincerely grateful to Dr. Jee Soo Park as well. It was thanks to Dr. Park that I was able to start my Ph.D. research. His unparalleled passion for research is something I truly wish to learn. His dedication throughout the process of my degree enabled me to complete my Ph.D. successfully.

Thanks are also due to Dr. Myung Eun Lee and Mr. Kwang-mo Shin from the Yonsei Urologic Oncology Lab. I am particularly grateful to Dr. Lee for conducting many experiments and enlightening me on areas I was unfamiliar with.

Lastly, I would like to thank my family. Although I often pretend to be busy and don't pay enough attention, I am genuinely thankful for their constant consideration and understanding.

TABLE OF CONTENTS

LIST OF FIGURES	iii
LIST OF TABLES	iv
ABSTRACT IN ENGLISH	v
1. INTRODUCTION	1
2. MATERIALS AND METHODS	2
2.1 Patients selection and tissues preparation	2
2.2 RNA extraction and sequencing	3
2.3 Analysis of RNA Sequencing and Differentially Expressed Gene (DEG) Selection	3
2.4 Network analysis	4
2.5 Immunohistochemistry and analysis of recurrence-free survival according to prostate stem cell antigen expression	4
2.6 Cell culture and PSCA expression in various RCC cell lines	5
2.7 Generation of PSCA knockdown in the 786-O cell line	5
2.8 Reverse transcription-quantitative PCR (RT-qPCR) analysis	6
2.9 Cell proliferation assay	7
2.10 Wound-healing assay	7
2.11 Invasion assay	8
2.12 Colony formation assay	8
2.13 RNA sequencing and DEG analysis in Control 786-O and siPSCA 786-O	8
2.14 Western blot analysis	9
2.15 Statistics	9
3. RESULTS	10
3.1 Characteristics of patients included in RNA-Seq	10
3.2 The result from the RNA-Seq and analysis	11
3.3 Differentially expressed genes	11
3.4 PSCA expression in ccRCC tissues and survival analysis according to PSCA expression	15
3.5 PSCA knockdown using siRNA in the 786-O cell line	17
3.6 Inhibition of cell proliferation, migration, invasion, and colony formation by PSCA downregulation in 786-O cells	18
3.7 Results of RNA-Seq with siPSCA and siControl 786-O	20
3.8 PSCA activates mTOR pathway and induces sensitivity to mTOR inhibitor	22
4. DISCUSSION	23

5. CONCLUSION	27
REFERENCES	28
ABSTRACT IN KOREAN	33

LIST OF FIGURES

<Fig 1> The results of RNA sequencing analysis	12
<Fig 2> PSCA expression in ccRCC tissues and recurrence-free survival according to PSCA expression	15
<Fig 3> PSCA expression in RCC cell lines and analysis of knockdown of PSCA with transfecting siRNA in 786-O	17
<Fig 4> Effects of PSCA knockdown on aggressiveness of 786-O cells	19
<Fig 5> GO enrichment analysis	20
<Fig 6> PSCA activates mTOR pathway and induces sensitivity to mTOR inhibitors	22
<Fig 7> Proposed model of PSCA/PGRN stimulating mTOR pathway	25

LIST OF TABLES

<Table 1> Designed target sequences for the siRNA for the PSCA	6
<Table 2> PCR primer sequences.	7
<Table 3> Clinicopathological characteristics of patients included in RNA sequencing	10
<Table 4> Significantly upregulated/downregulated genes in small ccRCC with or without aggressive characteristics	14
<Table 5> Clinicopathologic characteristics of 50 patients included in immunohistochemistry	16
<Table 6> Significantly upregulated/downregulated genes in siPSCA 786-O to siControl 786-O ..	21

ABSTRACT

Discovery of Biomarkers for Predicting Aggressive Small Renal Cell Cancer

Background:

Small renal cell cancer (RCC), confined to the kidney and measuring less than 4 cm, is increasingly diagnosed due to the widespread use of imaging tests such as computed tomography and ultrasound. Small RCC is typically slow-growing and has a favorable prognosis; therefore, various guidelines suggest active surveillance as a treatment option. However, some cases exhibit aggressive characteristics such as synchronous metastasis or recurrence. Therefore, markers that can predict aggressive small RCC and help identify patients requiring active treatment are needed.

Methods:

We obtained formalin-fixed paraffin-embedded samples from five patients with aggressive clear cell RCC (ccRCC) and five with characteristics similar to those of non-aggressive ccRCC who underwent partial or radical nephrectomy between December 2018 and September 2021. Aggressive ccRCC was defined as the one with synchronous metastasis or recurrence. We conducted RNA sequencing and analyzed differentially expressed genes (DEGs) in the samples from 10 patients. Additionally, we selected 50 patients who had undergone surgery for small ccRCCs between January and December 2014. Immunohistochemistry (IHC) was performed to evaluate the association between the expression of prostate stem cell antigen (PSCA; identified as a DEG) and aggressiveness of small ccRCC. IHC results were categorized as follows: the negative group included expression intensities of 0 (negative) and 1 (weak), whereas the positive group included intensities of 2 (moderate) and 3 (strong). Based on the IHC results, we analyzed recurrence-free survival (RFS) according to PSCA expression using the Kaplan–Meier curve and log-rank test. We knocked down PSCA in 786-O cells using small interfering RNA and conducted proliferation, migration, invasion, and colony formation assays. After PSCA knockdown, we evaluated the expression levels of key proteins in the mTOR pathway that are thought to be associated with PSCA. Additionally, we compared the expression of phosphorylated PI3K (p-PI3K), AKT, p-AKT, mTOR, and p-mTOR (key proteins in the mTOR pathway), which is considered a mechanism of PSCA.

Results:

In total, 418 genes were differentially expressed with absolute fold changes of ≥ 2 and p-values < 0.05 . After adjustment, PSCA expression was shown to be significantly upregulated. The proportion of aggressive small ccRCCs was significantly higher in the PSCA-positive group than in the PSCA-negative group. RFS was poorer in the PSCA-positive group than in the PSCA-negative group. PSCA knockdown in 786-O cells inhibited proliferation, migration, invasion, and colony formation. Additionally, when PSCA was knocked down, the levels of p-PI3K/PI3K, p-AKT/AKT, and p-mTOR/mTOR decreased, suggesting that PSCA activated the mTOR pathway, thereby acquiring aggressiveness. Compared with 786-O cells with PSCA knockdown control 786-O cells with upregulated PSCA, showed increased sensitivity to the mTOR inhibitor, everolimus.

Conclusions:

Our study showed that PSCA might be a potential biomarker for predicting aggressive small ccRCCs. Using RNA sequencing and immunohistochemistry, we found that PSCA upregulation was associated with aggressive small ccRCCs and poor RFS. Functional experiments showed that PSCA knockdown inhibited cancer-related processes such as proliferation, migration, and invasion. Mechanistically, PSCA appears to promote cancer aggressiveness by activating the mTOR pathway, as shown by the reduced levels of p-PI3K, p-AKT, and p-mTOR upon PSCA knockdown. These findings provide insights into ccRCC molecular dynamics and suggest potential therapeutic targets for the PSCA pathway.

Key words : renal cell cancer, biomarker, metastasis, recurrence

1. Introduction

Renal cell cancer (RCC) accounts for the majority of kidney cancer cases (80–90%) (1). The prevalence of RCC has increased over the last several decades owing to the widespread use of cross-sectional imaging. Among the newly diagnosed cases, approximately 70% fall into the category of small RCC, which refers to tumors that are less than 4 cm in size and are localized to the kidney (2). Several guidelines suggest partial nephrectomy, ablative therapy, or active surveillance (AS) as treatment options for T1a RCC (3, 4).

AS involves monitoring the tumor size and characteristics through serial imaging. Intervention is deferred unless an evidence of clinical progression is observed during the follow-up period (5). Although no established criteria exists for the application of AS in RCC, it may be considered for patients with small tumors measuring less than 2 to 3 cm, advanced age, or multiple comorbidities (1, 3, 4). The rationale for AS is largely based on clinical experience. Among renal masses smaller than 4 cm, known as small renal masses (SRM), approximately 20–30% are reported as benign tumors. Even if confirmed as malignant, most RCCs grow slowly. For instance, Pierorazio et al. (6) reported no instances of metastasis during a 2.1-year follow-up in 223 patients with RCC managed with AS. Another rationale for AS is the indolent growth rate of SRM. Various meta-analyses examining growth rates have shown that these masses exhibit annual growth rates of 0.2 to 0.3 cm, with 23–33% demonstrating no growth while under AS (7).

T1a RCC is generally associated with good prognosis. However, some patients exhibit aggressive characteristics. Jewett et al. (8) observed metastases in 1.3% of 151 tumors over a 28-month follow-up period. Meanwhile, Brunocilla et al. (9) found that 2 of 60 patients (3.4%) with a longer follow-up of 88.5 months died from RCC. They concluded that patients with a faster tumor growth index have a higher risk of disease progression. Furthermore, several studies have reported that delayed recurrence after 5 years is common, suggesting the need for follow up even after 5 years for high-risk patients (10–13). Consequently, the guidelines suggest selectively performing follow-up imaging tests even after 5 years. However, it has been proposed that follow-up imaging tests should be selectively performed based on the patient's preference and attending physician's judgment, rather than solely relying on objective tumor characteristics or predictive markers for the risk of recurrence. (1, 3).

Considering the aggressive characteristics of small RCCs, it is imperative to assess patients who require active treatment and those who should be closely monitored over an extended period. Previous studies have examined various factors associated with the diagnosis and prognosis of RCCs. Specific hematologic markers, such as serum calcium,

C-reactive protein, and neutrophil-to-lymphocyte ratio are associated with RCC prognosis (14-17). However, these markers are not indicative of small RCCs and have limited diagnostic value. Other studies have focused on biomarkers based on genes associated with RCC prognosis, particularly in T1 RCC. Ahn et al. (18) performed whole exome sequencing on formalin-fixed paraffin-embedded (FFPE) samples obtained from 10 patients with clear cell RCC (ccRCC), all with tumors measuring ≤ 7 cm and with synchronous metastasis, and subsequently expanded their investigation to include The Cancer Genome Atlas (TCGA) ccRCC dataset. Their findings highlighted that FOXC2 and CLIP4 are significant predictors of synchronous metastasis. Another study corroborated these findings, reporting significantly reduced levels of FOXC2, PBRM1, and BAP1 in aggressive ccRCCs measuring >7 cm (19). However, most previous studies included RCCs measuring >7 cm, resulting in a median tumor size of 3 to 4 cm or larger. Consequently, these studies also encompassed relatively large tumors, thereby limiting the ability to establish a treatment strategy for patients with small RCC based on these findings. Hence, it is imperative to identify the genetic characteristics that can accurately predict the prognosis of small RCCs. The objective of this study was to identify biomarkers that can predict aggressive features in patients with small ccRCCs.

2. Materials and Methods

2.1. Patients selection and tissues preparation

We reviewed clinical information obtained from an RCC cohort that was prospectively collected from December 2018 to September 2021. The cohort included patients who underwent surgical interventions for RCC. Clinical data and tumor tissue and blood samples were meticulously collected. From this cohort, we selected five patients with aggressive small ccRCCs. Aggressive tumors were defined as those demonstrating synchronous metastasis or recurrence, where synchronous metastasis was identified within 3 months of the primary RCC diagnosis. Additionally, we carefully matched this aggressive subgroup with five patients exhibiting non-aggressive characteristics, considering factors such as sex, age, tumor grade, and tumor size.

Formalin-fixed paraffin-embedded (FFPE) sections from 10 patients with ccRCC were procured from the archives of the Department of Pathology at Yonsei University College of Medicine. The identification of non-tumor elements within these sections was

based on hematoxylin and eosin-stained slides, and every sample was meticulously reviewed by a urologic pathologist. Subsequently, the samples were cut into 20 μ m sections and transferred to extraction tubes for further processing.

2.2. Patients selection and tissues preparation

RNA was extracted using the FFPE RNeasy kit (Qiagen, Gaithersburg, MD, USA) from 10 FFPE sections. 100 ng of RNA was used to construct a sequencing library using the TruSeq RNA Access library prep kit (Illumina, San Diego, CA, USA) according to the manufacturer's protocols.

Quantification of the sequencing libraries was achieved using the Kapa Biosystems Library Quantification Kit tailored for Illumina's sequencing platforms, following the qPCR Quantification Protocol Guide (KapaBiosystems, Wilmington, MA, USA, Catalog #KK4854). The libraries' quality was assessed using the TapeStation D1000 ScreenTape by Agilent Technologies, Palo Alto, CA, USA (Catalog # 5067-5582). These indexed libraries were then processed on the Illumina NovaSeq 6000 system for paired-end sequencing (2 X 101 bp). All these procedures were conducted by Macrogen Incorporated.

2.3. Analysis of RNA Sequencing and Differentially Expressed Gene (DEG) Selection

Paired-end sequencing (101 bp) was used to generate reads from the cDNA libraries, which were then trimmed and aligned to the UCSC hg19 reference human genome. Subsequent transcriptome assembly involved the categorization of known, novel, and alternatively spliced transcripts. Transcript and gene expression levels were quantified using read counts (number of reads aligned to a gene) and fragments per kilobase of exon per million mapped fragments (FPKM) values for each sample. To differentiate between DEGs of the aggressive and non-aggressive ccRCC groups, an initial filter was applied to exclude genes with zero read counts in more than one sample.

For DEGs, a complete linkage method and Euclidean distance were used to perform unsupervised hierarchical clustering analysis to discern patterns of gene expression. Additionally, principal component analysis was employed to simplify the complexity of the dataset by converting it into a set of new variables that encapsulated the essential aspects of the data. Macrogen Inc. carried out all data analyses and visualization of DEGs

using R version 3.5.1.

2.4. Network analysis

To identify key biological networks and hub genes associated with aggressive versus non-aggressive small ccRCCs, we performed a weighted gene co-expression network analysis (WGCNA) using the WGCNA package in R. We constructed an unsigned network with soft-thresholding power determined based on the scale-free topology criterion. By detecting the modules of highly correlated genes, we assessed the module significance based on their correlation with aggressiveness. Furthermore, we identified hub genes within the significant modules based on their module membership and gene significance values.

2.5. Immunohistochemistry and Analysis of Recurrence-Free Survival According to Prostate Stem Cell Antigen Expression

We conducted immunohistochemistry for prostate stem cell antigen (PSCA) using mouse anti-PSCA monoclonal antibody (1:100; sc-80654, Santa Cruz Biotechnology, Inc., Santa Cruz, CA, USA). We reviewed the medical records of patients who underwent partial or radical nephrectomy for small ccRCC between January 2014 and December 2014. We identified 11 patients with aggressive characteristics and 39 with non-aggressive characteristics who were followed up for more than 5 years. FFPE specimens from these 50 patients were cut into 4- μ m-thick sections and placed on Superfrost Plus microscope slides (Thermo Fisher Scientific). The sections were deparaffinized using EZ Prep (Ventana) for 8 min at 75 °C. Antigen retrieval was performed in cell conditioning solution (high pH CC1 standard) for 60 min at 100 °C. The endogenous peroxidase activity was blocked using a 3% H₂O₂ DAB inhibitor for 4 min at 37 °C. Subsequently, the slides were incubated with primary antibodies for 32 min at 37 °C, followed by incubation with a secondary antibody (Universal HRP Multimer) for 8 min at the same temperature. The slides were then treated with DAB + H₂O₂ substrate for 8 min and counterstained with hematoxylin II and bluing reagent at 37 °C. Tris buffer (pH 7.6) was used as the wash solution throughout the process. Finally, the slides were evaluated using light microscopy at $\times 100$ to $\times 400$ magnification to document the staining intensity, which was categorized as 0 (negative), 1 (weak), 2 (moderate), or 3 (strong). Immunohistochemical staining intensities of 0 and 1 were classified as PSCA-negative,

whereas intensities of 2 and 3 were classified as PSCA-positive. We used the Kaplan–Meier method with log-rank tests to estimate and compare progression-free survival between the PSCA-positive and-negative groups.

2.6. Cell culture and PSCA expression in various RCC cell lines

We obtained the human RCC cell lines including 786-O, A498, ACHN, Caki-1, 769-P, A704, SW156, and Caki-2, as well as the murine RCC cell line, Renca from the American Type Culture Collection (Rockville, MD, USA). UOK120 and UOK146 cell lines were provided by Dr. W. Marston Linehan (National Cancer Institute, Bethesda, MD, USA). The S-TFE cell lines were obtained from the Riken Cell Bank (Tsukuba, Japan). These cell lines were cultured in Roswell Park Memorial Institute 1640, Dulbecco's Modified Eagle Medium, or Eagle's Minimum Essential Medium supplemented with 10% fetal bovine serum (FBS) (Gibco; Thermo Fisher Scientific, Waltham, MA, USA) and 1% penicillin-streptomycin (Sigma-Aldrich, St. Louis, MO, USA) at 37 °C in a humidified atmosphere containing 5% CO₂. We performed Western blot analysis to verify the expression of PSCA in these cell lines. Western blotting analysis is described in detail in Section II.13.

2.7. Generation of PSCA knockdown in the 786-O cell line

We used small interfering RNA (siRNA) to knockdown PSCA in the 786-O cell line, a representative ccRCC cell line with a high expression level of PSCA, confirmed using Western blotting. The 786-O cells were transfected with ON-TARGET plus Human PSCA siRNA (Dharmacon, Lafayette, CO, USA) or a control ON-TARGET plus a non-targeting siRNA pool (Dharmacon) using Lipofectamine RNAiMAX (Invitrogen) as the siRNA delivery vehicle. The siRNA sequences are listed in Table 1. For PSCA knockdown, 786-O cells were seeded in six-well plates at a density of 6×10^5 cells per well. After 24 h of incubation at 37 °C, the cells were transfected with 50 nM specific PSCA siRNAs or scrambled siRNA using Lipofectamine RNAiMAX and serum-free Opti-MEM. A complete medium containing 10% FBS was added to the final volume of 2.5 mL/well.

Table 1. Designed target sequences for the siRNA for the PSCA

Primer	Sequence (5' → 3')
siPSCA(J-003697-09)	GGACAGGAGUCGACGUGAG
siPSCA(J-003697-10)	CGGUAAAGGCUGAGAUGAA
siPSCA(J-003697-11)	UGGAUGACUCACAGGACUA
siPSCA(J-003697-12)	ACGCAAGUCUGACCAUGUA

2.8. Reverse transcription-quantitative PCR (RT-qPCR) analysis

To verify the extent of PSCA knockdown at the RNA level after transfecting 786-O cells with PSCA-targeted siRNA, we conducted RT-qPCR. Total RNA was extracted from cells using TRIzol reagent (Invitrogen, Carlsbad, CA, USA) and reverse-transcribed into first-strand cDNA using a Maxime RT-PCR PreMix Kit (iNtRON Biotechnology, Seongnam, Gyeonggi-Do, Korea) according to the manufacturer's protocol. The qRT-PCR was performed using Power SYBR® Green Master Mix (Applied Biosystems, Foster City, CA, USA) in a 10- μ L reaction solution comprising 5 μ L of SYBR® Green Master PCR mix, 1 μ L of each forward and reverse primer (10 pmol), 1 μ L of diluted cDNA template, and sterile distilled water. The PCR primer sequences are listed in Table 2. Conditions for amplification were as follows: initial denaturation at 95 °C for 10 min; 40 cycles of denaturation at 95 °C for 15 s, annealing at 58 °C for 30 s, and elongation at 72 °C for 30 s; final elongation at 72 °C for 5 min. qRT-PCR was performed using the ABI StepOnePlus Real-Time PCR System (Applied Biosystems). Data were normalized to GAPDH gene expression, and the relative gene expression was analyzed using the $2^{-\Delta\Delta CT}$ method. The qRT-PCR experiments were repeated at least thrice.

Table 2. PCR primer sequences

Primer	Sequence (5' → 3')
PSCA-1 Forward	CACTGCCCTGCTGTGCTACT
PSCA-1-Reverse	CGCGGTCCAGCACTGCTCCC
PSCA-2-Forward	CCTAACGCAAGTCTGACCATGTATG
PSCA-2-Reverse	TGCAGGCGGATCTGTGTCACTA
GAPDH-Forward	ACCCACTCCTCCACCTTTGA
GAPDH-Reverse	CTGTTGCTGTAGCCAAATTCGT

2.9. Cell proliferation assay

Cell proliferation was assessed based on PSCA expression. The cells were seeded in 96-well culture plates at a density of 5×10^3 cells/well. Cell proliferation was determined at 24–72 h using the Cell Counting Kit-8 (DOJINDO, Tokyo, Japan) according to the manufacturer's instructions. Absorbance was measured at 450 nm using a VersaMax Microplate Reader (Molecular Devices, Sunnyvale, CA, USA). All experiments were performed in triplicates. Values were calculated as the mean and standard deviation (SD) of the percentage change induced by each siRNA compared to control.

2.10. Wound-healing assay

To evaluate the role of PSCA in cell migration, 786-O cells were transfected with siPSCA for 24 h. Thereafter, the cells were resuspended and seeded in six-well plates at a density of 1×10^6 cells/well, and 2 mL of culture medium supplemented with 10% FBS was added. Cells were grown to 90% confluence, and then, a uniform and consistent wound was scraped at the bottom of the six-well plate with a 200 μ L plastic pipette tip (time set as 0 h). The scratch time was designated as 0 h, and the cells were allowed to migrate into the gap. The cells were then incubated for 24 h in culture medium and photographed under an inverted microscope at 0 and 24 h. The Image J software (National Institutes of Health, Bethesda, Maryland, USA) was used to calculate the

healing area, and the healing rate was calculated as follows: (initial scratch width–existing scratch width)/initial scratch width × 100%.

2.11. Invasion assay

The invasion ability of 786-O cells, according to PSCA, was measured using the CytoSelect™ 24-Well Cell Invasion Assay kit (Cell Biolabs, San Diego, CA, USA). The 786-O cells were transfected with siRNA to PSCA for 24 h, and non-targeting siRNA (control) was used as the control. Control and transfected cells (1×10^4) were resuspended in serum-free medium and seeded in the upper chamber for invasion assay. Subsequently, a medium containing 10% FBS was added to the lower chambers. Following a 24-h incubation, the cells from the upper compartments were scraped off with cotton swabs, and the cells that invaded the lower surface of the membrane were fixed with pre-cooled methanol at room temperature for 20 min and stained with 0.1% crystal violet at room temperature for 20 min. The stained cells were quantified at 560 nm optical density after extraction using a VersaMax Microplate Reader (Molecular Devices).

2.12. Colony formation assay

We also evaluated the colony-forming ability of 786-O cells. Cells were transfected with siRNA against PSCA for 24 h, and non-targeting siRNA (control) was used as the control. Subsequently, 1000 cells/well were seeded in six-well plates and cultured for 9 days. The colonies were fixed with methanol and stained with 0.5% crystal violet. A cell colony was defined as a group of at least 50 cells, and the percentage of plating efficiency was measured using the Image J software.

2.13. RNA sequencing and DEG analysis in Control 786-O and siPSCA 786-O

To investigate the differences in downstream pathways resulting from PSCA expression, RNA was extracted from control 786-O cells and siPSCA-786-O (786-O cells with PSCA knockdown using PSCA siRNA). And then, RNA sequencing and DEG

analysis were performed. This process was carried out in the same method as described in sections II.2 and II.3.

2.14. Western blot analysis

Western blotting was performed to compare the expression of phosphorylated PI3K (p-PI3K), AKT, p-AKT, mTOR, and p-mTOR, which are key proteins in the mTOR pathway. The process of Western blotting for PSCA (described in II.6) and the three proteins was as follows: proteins were extracted using lysis buffer, a mixture of RIPA buffer, and protease inhibitor cocktails (Sigma-Aldrich, St. Louis, MO, USA). The protein content was determined using a BCA protein assay kit (Pierce, Rockford, IL, USA). Equal amounts of denatured proteins were separated by electrophoresis on sodium dodecyl sulfate–polyacrylamide gel electrophoresis gels, transferred to a polyvinylidene fluoride membrane, and blocked with 5% bovine serum albumin in tris buffered saline containing 0.1% Tween-20. The membranes were probed with the following primary antibodies: anti-PSCA (#137936, Abcam, Cambridge, MA, USA) diluted 1:1000, anti-p-PI3K (#4228, Cell Signaling Technology) diluted 1:1000, anti-PI3K (#4292, Cell Signaling Technology) diluted 1:1000, anti-p-AKT (#9271, Cell Signaling Technology) diluted 1:1000, anti-AKT (#9272, Cell Signaling Technology) diluted 1:1000, anti-p-mTOR (#2971, Cell Signaling Technology) diluted 1:1000, anti-mTOR (#2972, Cell Signaling Technology) diluted 1:1000, and anti-b-actin (#47778, Santa Cruz Biotechnology) diluted 1:5000, and subsequently incubated with horse radish peroxidase-conjugated secondary antibody (cell signaling technology). To detect reactive bands, the membranes were examined using the ECL Prime Western Blotting Detection System (GE Healthcare, Amersham, UK) and LAS-3000 (Fujifilm, Tokyo, Japan).

2.15. Statistics

Statistical analyses were performed using GraphPad Prism version 5.0 software (GraphPad Software, San Diego, CA, USA). The data are presented as mean \pm SD for all figure panels in which error bars are shown. We compared the rate of aggressive ccRCC between the PSCA-positive and PSCA-negative groups using the chi-squared test. Additionally, we used the Kaplan–Meier method with log-rank tests to estimate and compare recurrence-free survival (RFS). Statistical significance was set at values of $p <$

0.05. All the statistical analyses were performed using STATA® version 15.1 (StataCorp LLC, College Station, TX, USA).

3. Results

3.1. Characteristics of patients included in RNA-Seq

Clinicopathologic information for the 10 patients included in the RNA sequencing study is presented in table 3. The mean tumor size was 3.0 ± 1.0 cm. Of the 5 patients with aggressive ccRCC, 3 had synchronous metastasis: 2 had lung metastasis and 1 had pancreatic metastasis. The remaining 2 patients experienced recurrence, with 1 recurrence in the lung and the other in the psoas muscle. There were no cancer-specific deaths.

Table 3. Clinicopathological characteristics of patients included in RNA sequencing

Aggressiveness	Patient ID	Sex	Age	Tumor Size (cm)	WHO/ISUP Grade	Synchronous metastatic site	Recurrence site
Y	A-1	M	54	2.8	3	bone	
Y	A-2	M	59	2.5	3		lung
Y	A-3	M	62	4.0	2		psoas muscle
Y	A-4	F	59	1.5	2	pancreas	
Y	A-5	M	65	3.8	4	bone	
N	NA-1	M	50	3.0	2		
N	NA-2	M	65	3.2	2		
N	NA-3	M	68	3.8	2		
N	NA-4	F	62	1.4	2		
N	NA-5	M	75	3.8	3		

WHO= World Health Organization; ISUP= International Society of Urological Pathology

3.2. The result from the RNA-Seq and analysis

RNA-seq analysis generated $56,909 \times 10^6$ bp from ccRCC samples with aggressive characteristics and $55,920 \times 10^6$ bp from ccRCC samples without aggressive characteristics. In total, 490×10^6 reads were mapped in ccRCC samples with aggressive characteristics, whereas 499×10^6 reads mapped to ccRCC samples without aggressive characteristics. No significant difference in the number of reads was observed between the two groups.

3.3. Differentially expressed genes

Of 22,840 genes included in the statistical analysis, 418 DEGs were identified. These DEGs met the criteria of an absolute fold change >2 and a raw p-value of <0.05 . Among these 418 DEGs, 332 were upregulated and 86 were downregulated, as shown in the volcano plot in Figure 1A. Unsupervised hierarchical clustering analysis (Figure 1B) and principal component analysis (Figure 1C) revealed clustering into two groups, although these groups were not perfectly distinct. The DEGs with the 10 lowest raw p-values are presented in Table 4. After adjustment using the Benjamini–Hochberg procedure, *PSCA* remained significantly upregulated. A network analysis was conducted to identify hub genes, and the results are shown in Figure 1D. *RBMX*, *PTPRN*, and *APLPI* were identified as the hub genes.

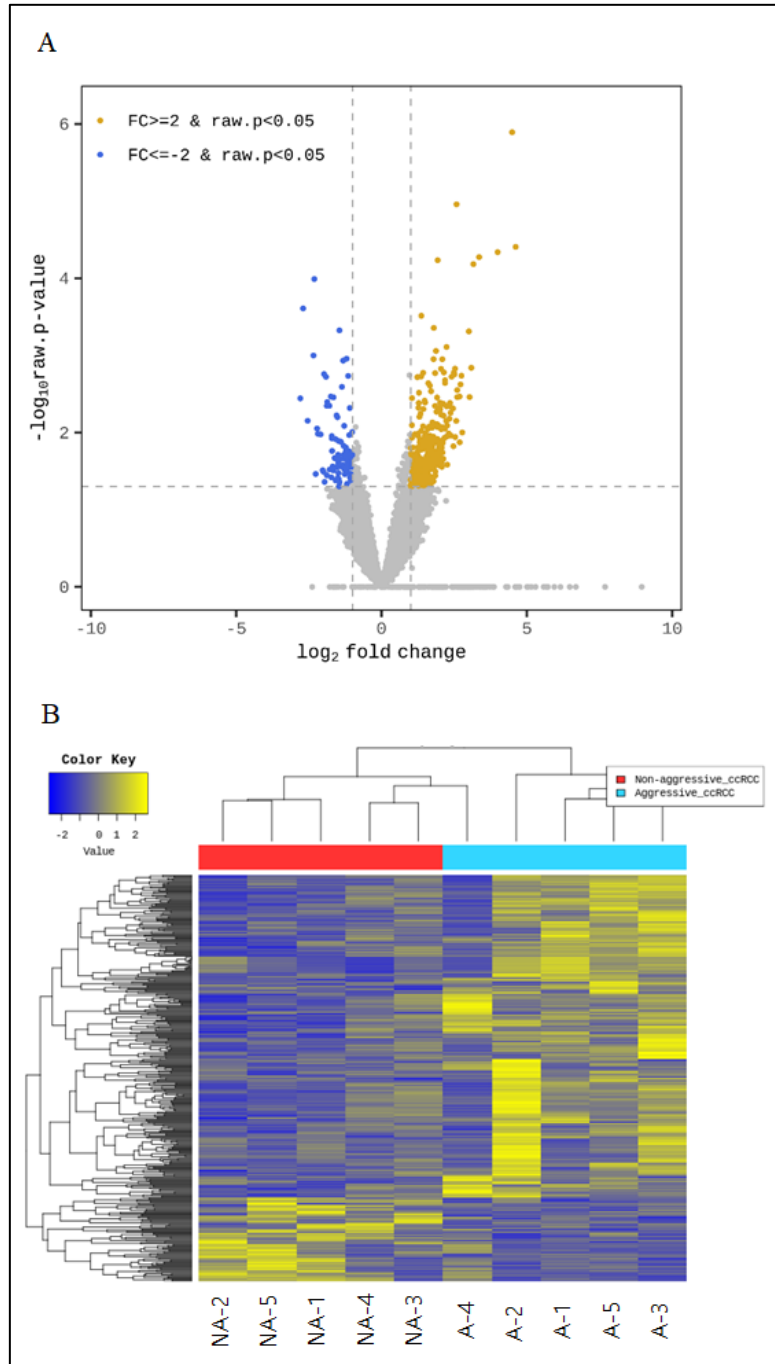


Figure 1 continued on next page

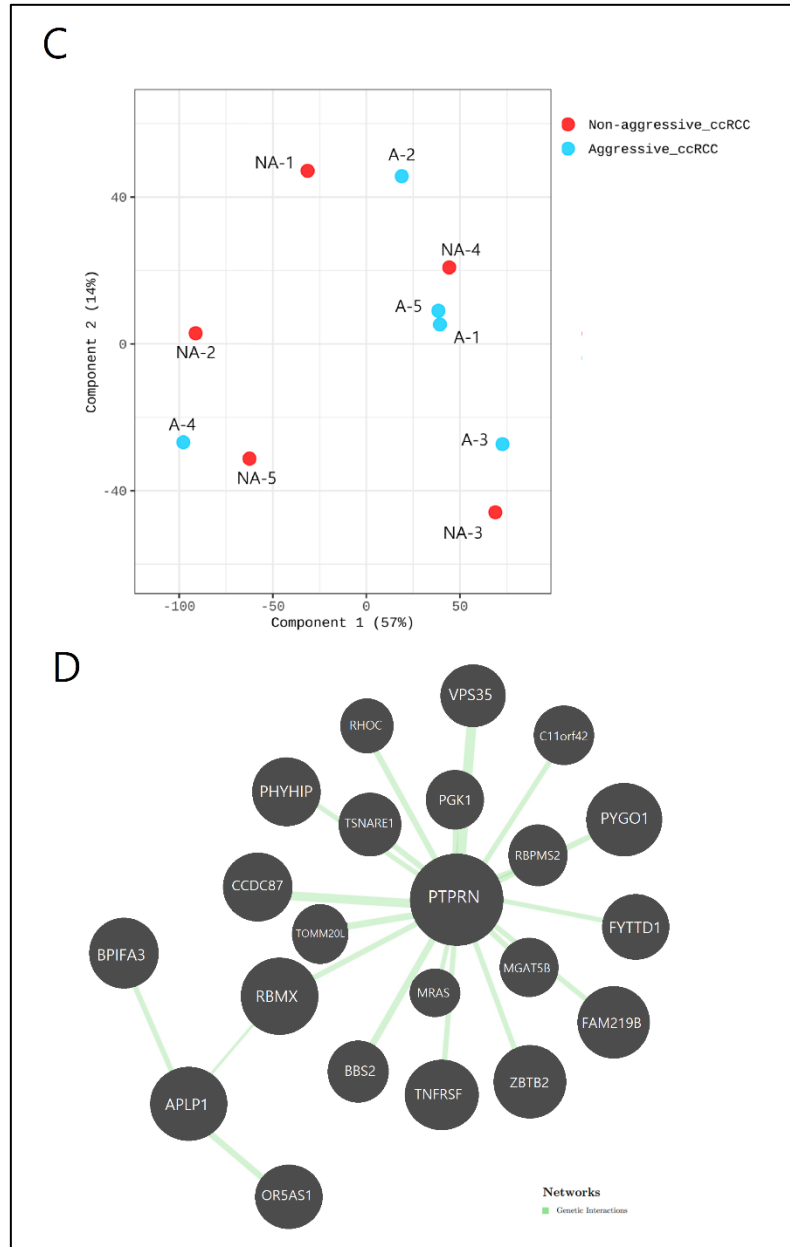


Figure 1. The results of RNA sequencing analysis. (A) Volcano plot comparing aggressive ccRCC and non-aggressive ccRCC. (B) Unsupervised hierarchical clustering analysis. (C) Principal component score plot. (D) Network analysis revealed *RBMX*, *PTPRN*, and *APLP1* as hub genes.

Table 4. Significantly upregulated/downregulated genes in small ccRCC with or without aggressive characteristics

Gene Symbol	Gene Title	Up- or downregulated	Log ₂ Fold Change	p-Value	Adj. p-value
<i>PSCA</i>	prostate stem cell antigen	upregulated	22.50	1.28 X 10 ⁻⁶	0.03
<i>S100P</i>	S100 calcium binding protein P	upregulated	5.98	1.10 X 10 ⁻⁵	0.12
<i>MSMP</i>	microseminoprotein, prostate associated	upregulated	24.50	3.92 x 10 ⁻⁵	0.21
<i>PTPRN</i>	protein tyrosine phosphatase receptor type N	upregulated	15.92	4.58 x 10 ⁻⁵	0.21
<i>SMOC1</i>	SPARC related modular calcium binding 1	upregulated	10.24	5.32 x 10 ⁻⁵	0.21
<i>PYCR1</i>	pyrroline-5-carboxylate reductase 1	upregulated	3.81	5.83 x 10 ⁻⁵	0.21
<i>MUC5AC</i>	mucin 5AC, oligomeric mucus/gel-forming	upregulated	8.94	6.56 x 10 ⁻⁵	0.21
<i>SYT8</i>	synaptotagmin 8	upregulated	2.58	3.06 x 10 ⁻⁴	0.69
<i>TMEM233</i>	transmembrane protein 233	downregulated	-2.73	4.73 x 10 ⁻⁴	0.85
<i>APLP1</i>	amyloid beta precursor like protein 1	upregulated	8.01	4.88 x 10 ⁻⁴	0.85

3.4. PSCA expression in ccRCC tissues and survival analysis according to PSCA expression

Western blotting was conducted to evaluate the expression of PSCA in non-aggressive ccRCC, aggressive ccRCC, and adjacent normal kidney tissues to determine its correlation with ccRCC aggressiveness. The results revealed that PSCA expression was higher in tumor tissues than in normal tissues. Furthermore, PSCA expression was higher in aggressive ccRCC than in non-aggressive ccRCC (Figure 2A).

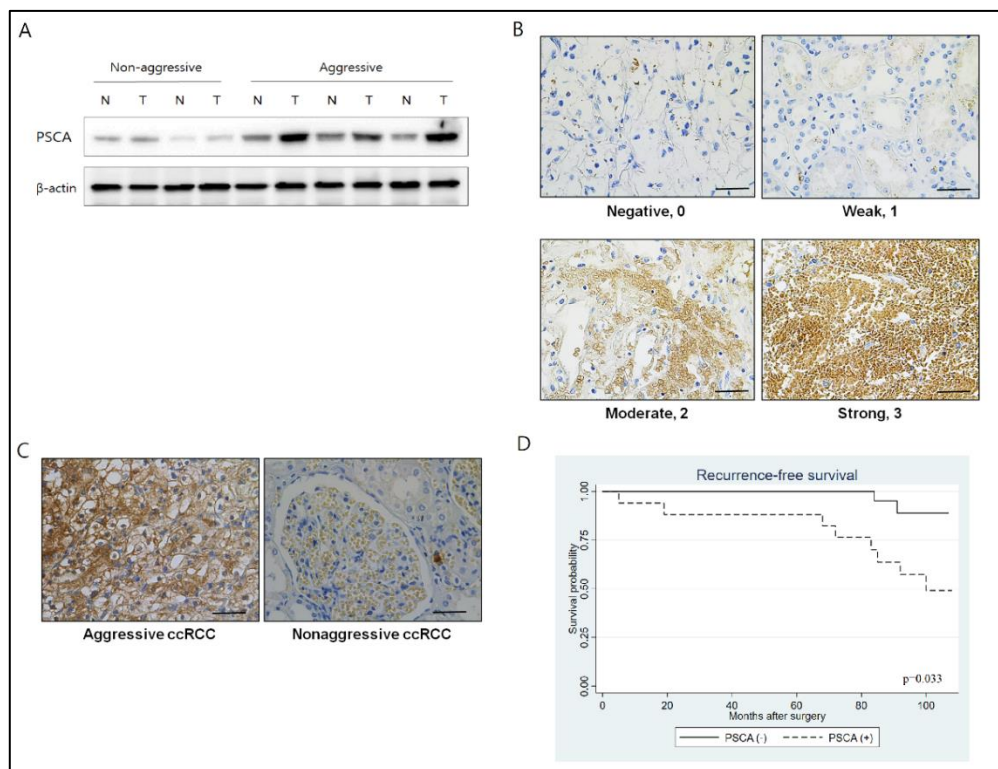


Figure 2. PSCA expression in ccRCC tissues and recurrence-free survival according to PSCA expression. (A) PSCA expression in non-aggressive ccRCC vs aggressive ccRCC and adjacent normal tissue. The bands in column N represents normal tissue, and column T represents tumor tissue. (B) IHC scoring according to PSCA expression level. (C) Representative IHC images (magnification x400) of aggressive and non-aggressive ccRCC. (D) Kaplan-Meier curve of recurrence-free survival according to PSCA expression

Immunohistochemical analysis was performed on FFPE samples obtained from the 50 patients. PSCA expression was categorized into four groups (Figure 2B). The representative images of aggressive and non-aggressive ccRCCs are shown in Figure 2C. The clinicopathological characteristics of the 50 patients are presented in Table 5. The proportion of aggressive RCC was significantly higher in the PSCA-positive group than in the PSCA-negative group (40.9% vs. 7.1%, $p=0.006$). Additionally, high-grade tumors were more common in the PSCA-positive group (63.6% vs. 28.6%, $p=0.021$). No statistically significant differences in sex, age, BMI, or tumor size were observed. Figure 2D illustrates the Kaplan–Meier curve for RFS based on PSCA expression. The 8-year RFS rate was 95.2% in the PSCA-negative group and 70.1% in the PSCA-positive group, indicating poor prognoses for patients who tested positive for PSCA ($p=0.033$).

Table 5. Clinicopathologic characteristics of 50 patients included in immunohistochemistry

	PSCA (-) 28	PSCA (+) 22	p-value
Sex, n (%)			0.070
Male	15 (53.6%)	18 (81.8%)	
Female	13 (46.4%)	4 (18.2%)	
Age (years)	60.6±6.16	60.7±8.45	0.972
BMI (Kg/m ²)	23.7±2.32	26.4±4.68	0.108
Tumor size (cm)	2.35±0.83	2.48±0.72	0.583
Fuhrman nuclear grade, n (%)			0.021
1 or 2	20 (71.4%)	8 (36.4%)	
3 or 4	8 (28.6%)	14 (63.6%)	
Aggressiveness, n (%)			0.006
None-aggressive	26 (92.9%)	13 (59.1%)	
Aggressive	2 (7.1%)	9 (40.9%)	
Synchronous metastasis, n (%)	0 (0.0%)	1 (4.5%)	0.440
Recurrence, n (%)	2 (7.1%)	8 (36.4%)	0.014

PSCA=prostate stem cell antigen; BMI=body mass index

3.5. PSCA knockdown using siRNA in the 786-O cell line

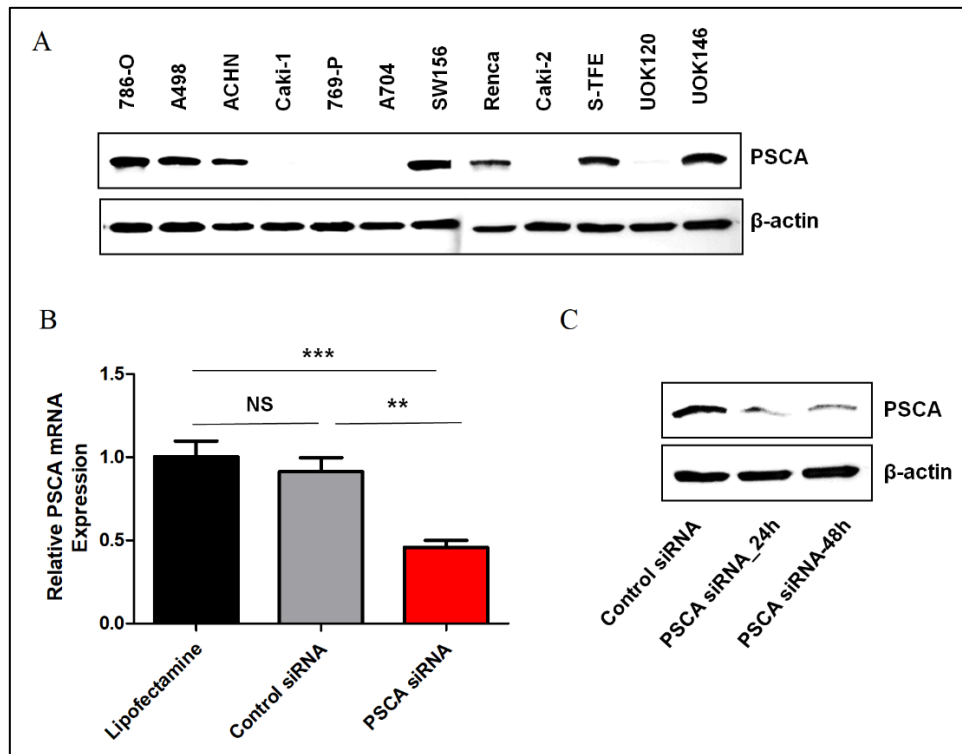


Figure 3. PSCA expression in RCC cell lines and analysis of knockdown of PSCA with transfecting siRNA in 786-O. (A) PSCA expression in various RCC cell line. (B) mRNA level of PSCA in 786-O cells when transfected with PSCA-targeted siRNA. (C) Protein level of PSCA in 786-O cells when transfected with PSCA-targeted siRNA.

Figure 3A illustrates the expression of PSCA in different RCC cell lines using Western blot analysis. Strong expression of PSCA was detected in 786-O, A498, ACHN, SW156, Renca, S-TFE, and UOK146 cells. Among these, the 786-O cell line, a representative ccRCC cell line known for its genetic characteristics, was chosen to establish a PSCA knockdown cell line for subsequent in vitro studies.

Following transfection of 786-O cells with PSCA siRNA (siPSCA-transfected 786-O cells), a notable reduction was observed in PSCA mRNA levels compared to 786-O cells transfected with a pool of siRNAs consisting of four non-targeting siRNAs (siControl-

transfected 786-O cells) and 786-O cells treated with Lipofectamine alone, as confirmed by qRT-PCR (Figure 3B). Western blot analysis yielded similar results, demonstrating a decrease in PSCA expression in siPSCA-transfected 786-O cells compared with that in siControl-transfected 786-O cells.

3.6 Inhibition of cell proliferation, migration, invasion, and colony formation by PSCA downregulation in 786-O cells

We transfected RCC cells (5000 cells/96-well plate) with 50 nM PSCA or a pool of control siRNAs. The rates of cell proliferation were measured 24 h post-transfection and every 24 h thereafter. Subsequently, cells were incubated every 24 h. As depicted in Figure 4A, 786-O cells transfected with siPSCA showed significantly inhibited proliferation up to 72 h post-transfection compared with cells transfected with siControl. The migration ability of 786-O cells was significantly impaired upon suppression of PSCA expression, as evidenced by a wound healing assay (Figure 4B). Additionally, the Transwell invasion assay revealed a decrease in invasiveness when PSCA was knocked down (Figure 4C). Furthermore, the knockdown of PSCA expression inhibited colony formation in 786-O cells (Figure 4D).

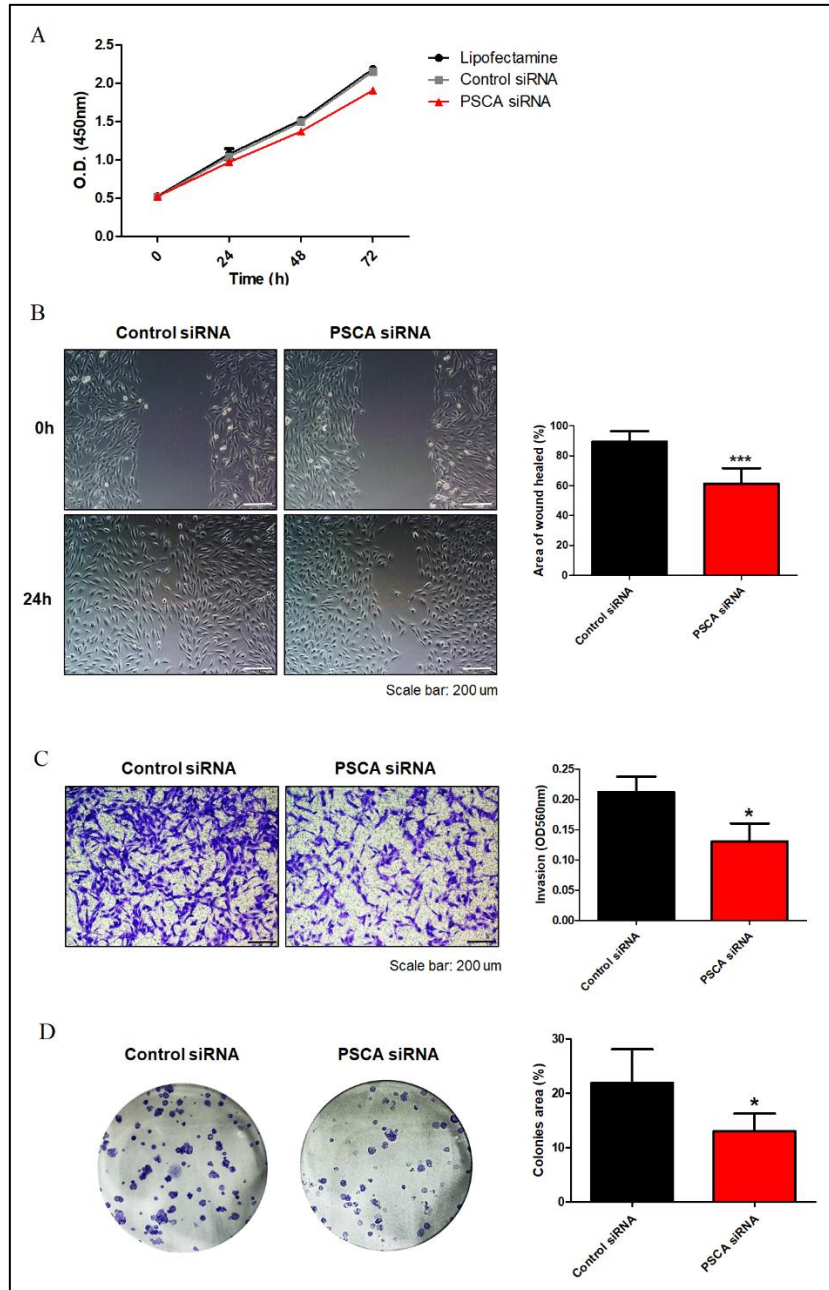


Figure 4. Effects of PSCA knockdown on aggressiveness of 786-O cells. PSCA knockdown inhibits proliferation (A), migration (B), invasion (C) and colony formation (D) of 786-O cells

3.7 Results of RNA-Seq with siPSCA and siControl 786-O

RNA-seq analysis generated $13,290 \times 10^6$ bp fragments from siControl 786-O cells and $13,340 \times 10^6$ bp fragments from siPSCA-transfected 786-O cells. In total, 127×10^6 reads were mapped in siControl-transfected PSCA, whereas 128×10^6 reads were mapped in siPSCA-transfected 786-O cells. No significant difference in the number of reads was observed between the two groups.

Of the 20,965 genes included in the statistical analyses, 316 genes were identified. After adjustment, five statistically significant DEGs were identified, as shown in table 6. Excluding ribosomal RNA and pseudogenes, *ATP5MF-PTCD1* and *TMEFF1* appeared to be significant DEGs. The GO enrichment analysis showed that the top three most enriched terms in the cellular component category were cell periphery, plasma membrane, and membrane (Figure 5).

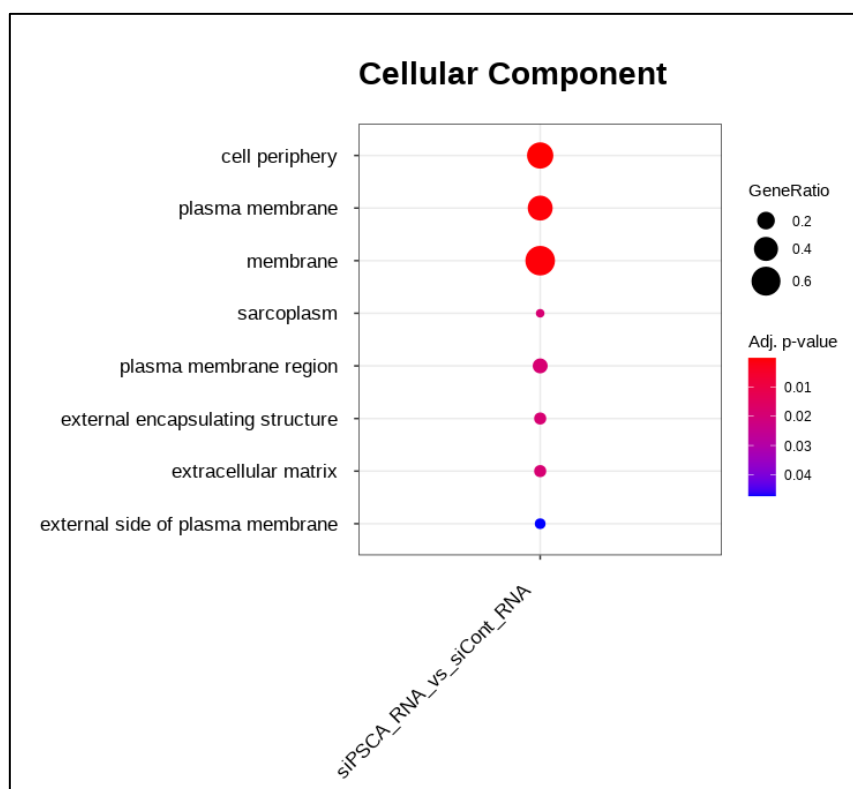


Figure 5. GO enrichment analysis. Top 7 terms in cellular component category

Table 6. Significantly upregulated/downregulated genes in siPSCA 786-O to siControl 786-O

Gene Symbol	Gene Title	Up- or downregulated	Log ₂ Fold Change	Adj. p-value
<i>RNA28SN1</i>	RNA, 28S ribosome N1	downregulated	-115.84	3.41 X 10 ⁻⁶
<i>RNA28SN1</i>	RNA, 28S ribosome N2	downregulated	-35.21	2.25 X 10 ⁻³
<i>ATP5MF-PTCD1</i>	ATP5MF-PTCD1 readthrough	upregulated	33.70	4.86 X 10 ⁻³
<i>ZRSR2P1</i>	ZRSR2 pseudogene 1	downregulated	-65.56	4.04 X 10 ⁻²
<i>TMEFF1</i>	Transmembrane protein with EGF like and two follistatin like domains 1	downregulated	-21.19	4.04 X 10 ⁻²

3.8 PSCA activates mTOR pathway and induces sensitivity to mTOR inhibitor

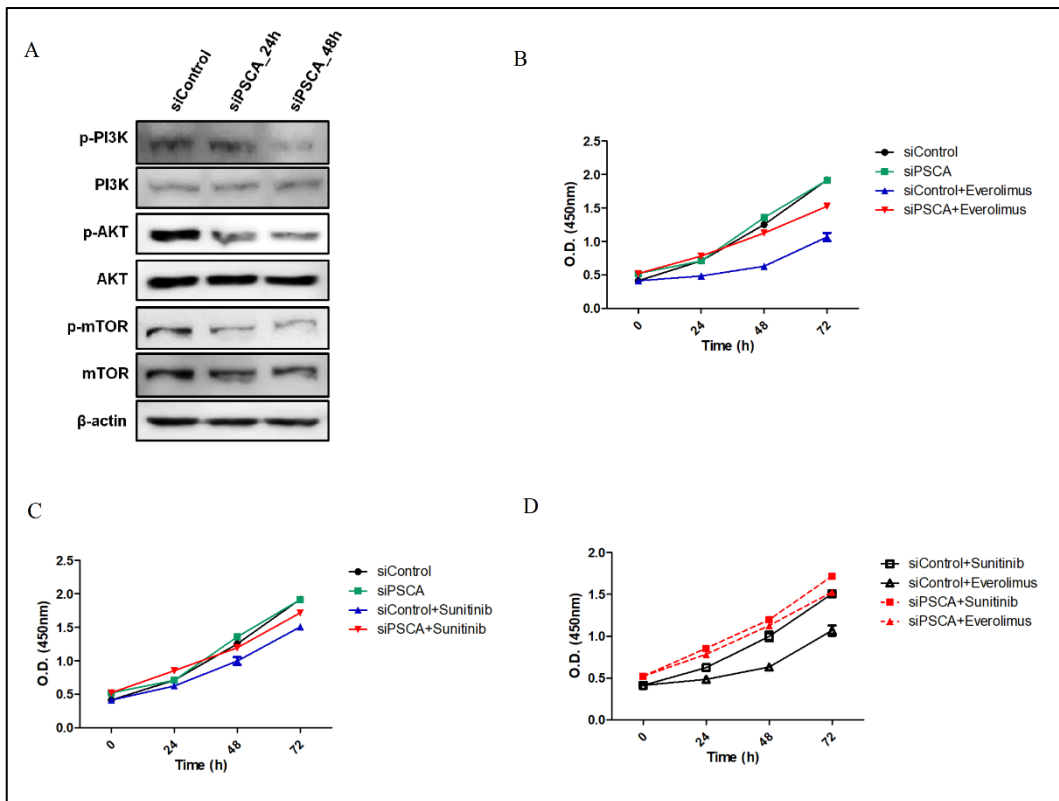


Figure 6. PSCA activates mTOR pathway and induces sensitivity to mTOR inhibitors. (A) Comparison of PI3K, AKT and mTOR levels between control and siPSCA 786-O. (B) Proliferation curves of 786-O cells transfected with the control siRNAs or PSCA siRNA following Everolimus treatment. (C) Proliferation curves of 786-O cells transfected with the control siRNAs or PSCA siRNA following Sunitinib treatment. (D) Proliferation curves of 786-O cells transfected with the control siRNAs or PSCA siRNA following Everolimus and Sunitinib treatment

Western blotting was performed to analyze the levels of proteins in the mTOR pathway, including p-PI3K, PI3K, p-AKT, AKT, p-mTOR, and mTOR, in relation to PSCA expression. The results indicated that the levels of p-PI3K/PI3K, p-AKT/AKT, and p-mTOR/mTOR decreased after transfection with siPSCA (Figure 5A). These findings suggest that PSCA may activate the mTOR pathway to promote aggressiveness.

To evaluate the therapeutic effect of the mTOR inhibitor everolimus on PSCA expression, we treated siPSCA-transfected 786-O cells and siControl-transfected 786-O cells with everolimus at various concentrations and measured cell viability over time. Figure 5B shows that siPSCA-transfected 786-O cells displayed resistance to everolimus compared to control 786-O cells. In contrast, no significant difference was observed in IC50 based on the PSCA knockdown status when treated with the tyrosine kinase inhibitor, sunitinib, which served as a control (Figure 5C and 5D). These results suggest that sensitivity to mTOR inhibitors is greater when the mTOR pathway is activated. Thus, the level of PSCA expression could potentially predict the therapeutic effect of mTOR inhibitors.

4. Discussion

PSCA is a glycosylphosphatidylinositol-anchored protein that belongs to the Thy-1/Ly-6 family. It is expressed in a various types of normal epithelia, including the skin, esophagus, stomach, gall bladder, kidney, and bladder (20, 21). However, the expression of PSCA in cancer cells depends on the epithelium of origin (22). Initially, PSCA was identified as a marker that is overexpressed in prostate cancer. Further research has revealed its upregulation in other types of tumors, such as bladder cancer, pancreatic cancer, hydatidiform mole, and ovarian mucinous tumors (22, 23). In RCC, a study by Essam et al. (24) reported a significant correlation between the gene expression level of PSCA and histological grade, clinicopathological stage, and prognosis in RCC.

In our study, PSCA emerged as a potential marker for predicting the aggressive characteristics of small ccRCCs. PSCA was identified as the sole DEG using RNA sequencing of FFPE samples from aggressive and non-aggressive small ccRCCs. Western blot analysis confirmed higher PSCA expression in cancer tissues than in normal kidney tissues, with aggressive ccRCC showing higher PSCA expression than that of non-aggressive ccRCC. Immunohistochemical staining revealed a higher rate of aggressive ccRCC and poorer recurrence-free survival in the PSCA-positive group. These findings suggest an association between PSCA expression and aggressiveness of small ccRCCs.

However, owing to the limited number of DEGs—specifically, only one DEG (PSCA)—exploring the mechanisms underlying PSCA's role was challenging. Typically, GO or KEGG pathways analyses were performed using multiple DEGs identified from RNA sequencing. Since there is limited research on the mechanisms of PSCA, elucidating how it contributes to the aggressiveness of small ccRCC remains difficult. To address these challenges, RNA was extracted from siPSCA-transfected 786-O and siControl 786-O cells, and RNA sequencing was performed. Five DEGs were identified, including *ATP5MF*, *PTCD1* and *TMEFF1*, which displayed potential functionality. *PTCD1* regulates mitochondrial RNA stability and translation, and previous studies have linked it to Alzheimer's disease (25). Downregulation of *PTCD1* in bladder cancer has also been associated with poor prognosis (26). *TMEFF1* has been extensively studied in the context of ovarian cancer and has been associated with a worse prognosis (27). Nie et al. (27) reported that *TMEFF1* promotes malignant behavior in ovarian cancer by modulating the MAPK and PI3K/AKT signaling pathways. The results of the GO analysis indicated differences only in the cell membrane and extracellular components. These findings provide limited insights into the mechanisms underlying PSCA.

Therefore, we aimed to develop a hypothesis regarding the pathway through which PSCA contributes to the aggressiveness of small ccRCCs, drawing upon previously published research and the mechanisms of genes that appear to be associated with PSCA. A previous study suggested an association between PSCA and the PI3K/AKT pathway in prostate cancer (28). Moreover, *PTPRN* and *APLP1*, identified as hub genes through network analysis, are suspected to be associated with the mTOR pathway (29, 30). *TMEFF1*, a DEG influenced by PSCA expression, activates the PI3K/AKT pathway. Although evidence for this association is weak, we conducted experiments to explore their relationship under the assumption that PSCA may be linked to the mTOR pathway. Our study revealed that downregulation of PSCA led to decreased levels of p-PI3K/PI3K, p-AKT/AKT, and p-mTOR/mTOR. These findings support the idea that PSCA enhances the aggressiveness of RCC by activating the PI3K/AKT/mTOR pathway.

However, there is limited knowledge regarding the mechanism by which the GPI-anchored protein, PSCA, transmits signals into the cell to activate the mTOR pathway. Saeki et al. (22) proposed that PSCA may form a complex with another protein to activate downstream targets; however, no proteins that bind to PSCA have been reported to date. Recently, Zhao et al. (31) suggested a potential interaction between PSCA and growth factor progranulin (PGRN) in prostate cancer. Their study found that downregulating PGRN and PSCA inhibits integrin- α 4 expression and adhesion to bone marrow endothelial cells in prostate cancer cells. They concluded that PSCA/PGRN promotes the adhesion of prostate cancer cells to bone marrow endothelial cells through the NF- κ B/integrin- α 4

pathways, thereby facilitating metastasis. Another study (32) reported that PGRN promotes tumorigenesis in cervical cancer via the mTOR signaling pathway. This study showed that PGRN enhances mTOR phosphorylation and activates its signaling in cervical mucosal epithelial and cervical cancer cells. They also found that tumor necrosis factor receptor 2 (TNFR2) was necessary for PGRN-stimulated mTOR signaling. Based on these results, we hypothesized that PSCA interacts with PGRN to activate the mTOR pathway via TNFR2 (Figure 7).

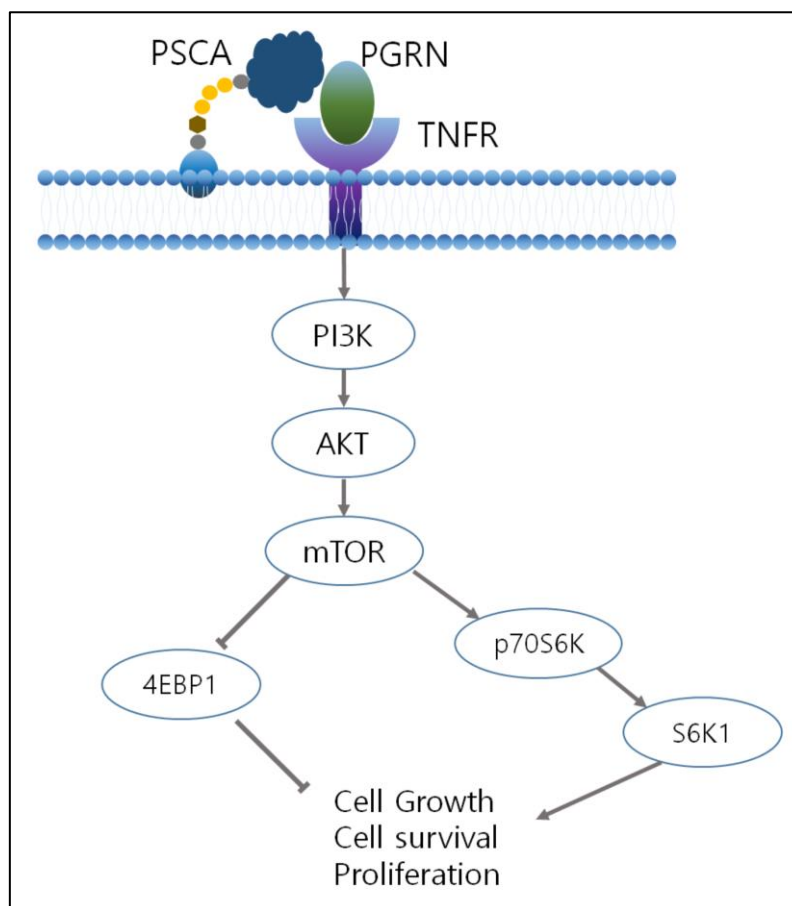


Figure 7. Proposed model of PSCA/PGRN stimulating mTOR pathway

Besides its role as a predictor of aggressiveness in small ccRCCs, PSCA has potential applications in the treatment of ccRCCs. We hypothesized that the effectiveness of mTOR

inhibitor treatment varies depending on the level of PSCA expression, considering its role in mTOR pathway activation. To investigate this, we evaluated the disparity in cell viability when 786-O cells were treated with the mTOR inhibitor, everolimus, compared with control 786-O cells, both with and without siPSCA treatment. These results indicated that PSCA knockdown resulted in increased resistance to everolimus in 786-O cells. These findings suggest that mTOR inhibitors may be more effective in treating PSCA-positive ccRCC. In contrast, sunitinib, another drug used in ccRCC treatment, did not display a similar dependence on PSCA expression levels. This result suggests that PSCA could serve as a marker for predicting the outcomes of mTOR inhibitor treatment. Another potential application of PSCA is its use as a therapeutic target. Hillerdal et al. (33) conducted preclinical experiments in a prostate cancer xenograft model and observed that chimeric antigen receptor (CAR) T cells targeting PSCA inhibits tumor growth and improves survival rates. This finding suggests that PSCA can serve as a therapeutic target in addition to being a biomarker. Currently, clinical trials are exploring the use of PSCA CAR-T cell therapy to treat metastatic prostate cancer (NCT03873805) and are evaluating its efficacy as a new treatment option. The positive outcomes of these trials indicate the potential applicability of PSCA CAR-T cell therapy for ccRCC.

This study has some limitation including the small number of patients from whom FFPE samples was obtained for RNA sequencing, as well as the short follow-up duration. Owing to the low rate of synchronous metastasis or recurrence in small ccRCCs, only five cases were confirmed as aggressive ccRCCs. Our initial aim was to identify hematological markers that could predict aggressive small ccRCCs and to verify them in these patients by comparing them with markers in blood samples. Since December 2018, we have prospectively collected tissue and blood samples from patients undergoing surgery for RCC. Hence, our study was conducted including patients admitted after December 2018 to compare PSCA levels in both tissue and blood samples. Recurrences in RCC have been reported even 5 years post-surgery, indicating the possibility of recurrence in the non-aggressive group in the future. Additionally, PSCA was found to be an inappropriate hematological marker, as it was not detected in the blood samples of female patients and showed a tendency to correlate with PSA levels in male patients. Therefore, PSCA is not a suitable hematological marker. However, it can be a valuable indicator for determining the appropriate course of action between active surveillance and active treatment in patients diagnosed with small ccRCCs through percutaneous renal biopsy. Furthermore, it is a useful marker for selecting patients who require aggressive long-term follow-up after surgery.

5. Conclusion

Our study highlights the significance of PSCA as a potential biomarker for predicting aggressive small ccRCCs. Through rigorous analysis following RNA sequencing, PSCA emerged as a promising candidate, which was further validated by immunohistochemistry and demonstrated higher rates of aggressive ccRCC and poorer recurrence-free survival in PSCA-positive individuals. Functional experiments revealed that PSCA knockdown effectively inhibited cell proliferation, migration, invasion, and colony formation, which are crucial cancer hallmarks. Mechanistically, our findings suggest that PSCA may drive aggressiveness through the activation of the mTOR pathway, as evidenced by decreased levels of p-PI3K, p-AKT, and p-mTOR upon PSCA knockdown. These results provide valuable insights into the molecular mechanisms underlying ccRCC aggressiveness and offer promising prospects for targeted therapeutic interventions targeting PSCA-mediated pathways.

References

1. Ljungberg B, Albiges L, Abu-Ghanem Y, Bedke J, Capitanio U, Dabestani S, et al. European Association of Urology Guidelines on Renal Cell Carcinoma: The 2022 Update. *Eur Urol* (2022) 82(4):399-410. doi:10.1016/j.eururo.2022.03.006
2. Bukavina L, Bensalah K, Bray F, Carlo M, Challacombe B, Karam JA, et al. Epidemiology of Renal Cell Carcinoma: 2022 Update. *Eur Urol* (2022) 82(5):529-42. doi:10.1016/j.eururo.2022.08.019
3. Campbell SC, Uzzo RG, Karam JA, Chang SS, Clark PE, Souter L. Renal Mass and Localized Renal Cancer: Evaluation, Management, and Follow-up: AUA Guideline: Part II. *J Urol* (2021) 206(2):209-18. doi:10.1097/ju.0000000000001912
4. NCCN Clinical Practice Guidelines in Oncology Kidney Cancer. (2024) Available online at: https://www.nccn.org/professionals/physician_gls/pdf/kidney.pdf (accessed April 1, 2024).
5. Stares M, Chauhan V, Moudgil-Joshi J, Kong QG, Malik J, Sundaramurthy A, et al. Initial active surveillance for patients with metastatic renal cell carcinoma: 10 years' experience at a regional cancer Centre. *Cancer Med* (2023) 12(5):5255-64. doi:10.1002/cam4.5330
6. Pierorazio PM, Johnson MH, Ball MW, Gorin MA, Trock BJ, Chang P, et al. Five-year analysis of a multi-institutional prospective clinical trial of delayed intervention and surveillance for small renal masses: the DISSRM registry. *Eur Urol* (2015) 68(3):408-15. doi:10.1016/j.eururo.2015.02.001
7. Ristau BT, Kutikov A, Uzzo RG, Smaldone MC. Active Surveillance for Small Renal Masses: When Less is More. *Eur Urol Focus* (2016) 2(6):660-8. doi:10.1016/j.euf.2017.04.004
8. Jewett MA, Mattar K, Basiuk J, Morash CG, Pautler SE, Siemens DR, et al. Active surveillance of small renal masses: progression patterns of early stage kidney cancer. *Eur Urol* (2011) 60(1):39-44. doi:10.1016/j.eururo.2011.03.030

9. Brunocilla E, Borghesi M, Schiavina R, Della Mora L, Dababneh H, La Manna G, et al. Small renal masses initially managed using active surveillance: results from a retrospective study with long-term follow-up. *Clin Genitourin Cancer* (2014) 12(3):178-81. doi:10.1016/j.clgc.2013.11.011
10. Shindo T, Masumori N, Kobayashi K, Fukuta F, Hirobe M, Tonooka A, et al. Long-term outcome of small, organ-confined renal cell carcinoma (RCC) is not always favourable. *BJU Int* (2013) 111(6):941-5. doi:10.1111/j.1464-410X.2012.11771.x
11. Dabestani S, Beisland C, Stewart GD, Bensalah K, Gudmundsson E, Lam TB, et al. Long-term Outcomes of Follow-up for Initially Localised Clear Cell Renal Cell Carcinoma: RECUR Database Analysis. *Eur Urol Focus* (2019) 5(5):857-66. doi:10.1016/j.euf.2018.02.010
12. Arai T, Sazuka T, Sato H, Kato M, Kamada S, Katsura S, et al. A clinical investigation of recurrence and lost follow-up after renal cell carcinoma surgery: a single-center, long-term, large cohort, retrospective study. *Int J Clin Oncol* (2022) 27(9):1467-76. doi:10.1007/s10147-022-02204-x
13. Almdalal T, Karlsson Rosenblad A, Hellstrom M, Kjellman A, Lindblad P, Lundstam S, et al. Predictive characteristics for disease recurrence and overall survival in non-metastatic clinical T1 renal cell carcinoma - results from the National Swedish Kidney Cancer Register. *Scand J Urol* (2023) 57(1-6):67-74. doi:10.1080/21681805.2022.2154383
14. Liu H, Tang K, Chen Z, Li Z, Meng X, Xia D. Comparison and development of preoperative systemic inflammation markers-based models for the prediction of unfavorable pathology in newly diagnosed clinical T1 renal cell carcinoma. *Pathol Res Pract* (2021) 225:153563. doi:10.1016/j.prp.2021.153563
15. Wang K, Dong L, Li S, Liu Y, Niu Y, Li G. CT features based preoperative predictors of aggressive pathology for clinical T1 solid renal cell carcinoma and the development of nomogram model. *BMC Cancer* (2024) 24(1):148. doi:10.1186/s12885-024-11870-

16. Elghiaty A, Kim J, Jang WS, Park JS, Heo JE, Rha KH, et al. Preoperative controlling nutritional status (CONUT) score as a novel immune-nutritional predictor of survival in non-metastatic clear cell renal cell carcinoma of ≤ 7 cm on preoperative imaging. *J Cancer Res Clin Oncol* (2019) 145(4):957-65. doi:10.1007/s00432-019-02846-x
17. Fukui S, Miyake M, Iida K, Onishi K, Hori S, Morizawa Y, et al. The Preoperative Predictive Factors for Pathological T3a Upstaging of Clinical T1 Renal Cell Carcinoma. *Diagnostics (Basel)* (2019) 9(3). doi:10.3390/diagnostics9030076
18. Ahn J, Han KS, Heo JH, Bang D, Kang YH, Jin HA, et al. FOXC2 and CLIP4 : a potential biomarker for synchronous metastasis of ≤ 7 -cm clear cell renal cell carcinomas. *Oncotarget* (2016) 7(32):51423-34. doi:10.18632/oncotarget.9842
19. Park JS, Lee HJ, Cho NH, Kim J, Jang WS, Heo JE, et al. Risk Prediction Tool for Aggressive Tumors in Clinical T1 Stage Clear Cell Renal Cell Carcinoma Using Molecular Biomarkers. *Comput Struct Biotechnol J* (2019) 17:371-7. doi:10.1016/j.csbj.2019.03.005
20. Bahrenberg G, Brauers A, Joost HG, Jakse G. Reduced expression of PSCA, a member of the LY-6 family of cell surface antigens, in bladder, esophagus, and stomach tumors. *Biochem Biophys Res Commun* (2000) 275(3):783-8. doi:10.1006/bbrc.2000.3393
21. de Nooij-van Dalen AG, van Dongen GA, Smeets SJ, Nieuwenhuis EJ, Stigter-van Walsum M, Snow GB, et al. Characterization of the human Ly-6 antigens, the newly annotated member Ly-6K included, as molecular markers for head-and-neck squamous cell carcinoma. *Int J Cancer* (2003) 103(6):768-74. doi:10.1002/ijc.10903
22. Saeki N, Gu J, Yoshida T, Wu X. Prostate stem cell antigen: a Jekyll and Hyde molecule? *Clin Cancer Res* (2010) 16(14):3533-8. doi:10.1158/1078-0432.Ccr-09-3169
23. Amara N, Palapattu GS, Schrage M, Gu Z, Thomas GV, Dorey F, et al. Prostate stem cell antigen is overexpressed in human transitional cell carcinoma. *Cancer Res* (2001) 61(12):4660-5.
24. Elsamman EM, Fukumori T, Tanimoto S, Nakanishi R, Takahashi M, Toida K, et al. The expression of prostate stem cell antigen in human clear cell renal cell carcinoma: a

- quantitative reverse transcriptase-polymerase chain reaction analysis. *BJU Int* (2006) 98(3):668-73. doi:10.1111/j.1464-410X.2006.06350.x
25. Fleck D, Phu L, Verschueren E, Hinkle T, Reichelt M, Bhangale T, et al. PTC1 Is Required for Mitochondrial Oxidative-Phosphorylation: Possible Genetic Association with Alzheimer's Disease. *J Neurosci* (2019) 39(24):4636-56. doi:10.1523/jneurosci.0116-19.2019
26. Zhou Z, Zhou Y, Zhou X, Huang Y, Cui Y, Zhang Y. Downregulation of PTC1 in Bladder Urothelial Carcinoma Predicts Poor Prognosis and Levels of Immune Infiltration. *J Oncol* (2022) 2022:1146186. doi:10.1155/2022/1146186
27. Nie X, Liu C, Guo Q, Zheng MJ, Gao LL, Li X, et al. TMEFF1 overexpression and its mechanism for tumor promotion in ovarian cancer. *Cancer Manag Res* (2019) 11:839-55. doi:10.2147/cmar.S186080
28. Li E, Liu L, Li F, Luo L, Zhao S, Wang J, et al. PSCA promotes prostate cancer proliferation and cell-cycle progression by up-regulating c-Myc. *Prostate* (2017) 77(16):1563-72. doi:10.1002/pros.23432
29. Wang D, Tang F, Liu X, Fan Y, Zheng Y, Zhuang H, et al. Expression and Tumor-Promoting Effect of Tyrosine Phosphatase Receptor Type N (PTPRN) in Human Glioma. *Front Oncol* (2021) 11:676287. doi:10.3389/fonc.2021.676287
30. Wu X, Chen S, Lu C. Amyloid precursor protein promotes the migration and invasion of breast cancer cells by regulating the MAPK signaling pathway. *Int J Mol Med* (2020) 45(1):162-74. doi:10.3892/ijmm.2019.4404
31. Zhao Z, Li E, Luo L, Zhao S, Liu L, Wang J, et al. A PSCA/PGRN-NF- κ B-Integrin- α 4 Axis Promotes Prostate Cancer Cell Adhesion to Bone Marrow Endothelium and Enhances Metastatic Potential. *Mol Cancer Res* (2020) 18(3):501-13. doi:10.1158/1541-7786.Mcr-19-0278
32. Feng T, Zheng L, Liu F, Xu X, Mao S, Wang X, et al. Growth factor progranulin promotes tumorigenesis of cervical cancer via PI3K/Akt/mTOR signaling pathway. *Oncotarget* (2016) 7(36):58381-95. doi:10.18632/oncotarget.11126

- 33.Hillerdal V, Ramachandran M, Leja J, Essand M. Systemic treatment with CAR-engineered T cells against PSCA delays subcutaneous tumor growth and prolongs survival of mice. *BMC Cancer* (2014) 14:30. doi:10.1186/1471-2407-14-30

Abstract in Korean

공격적인 T1a 병기 신세포암 예측을 위한 바이오마커 탐색

작은 신세포암은 컴퓨터 단층 촬영(CT)과 초음파와 같은 영상 진단 검사들이 널리 사용됨에 따라 점점 더 많이 진단되고 있다. 4cm 이하이면서 신장에 국한된 작은 신세포암은 일반적으로 천천히 자라고 예후가 좋은 것으로 알려져 있어, 다양한 가이드라인에서 능동감시를 치료 옵션 중 하나로 제안하고 있다. 그러나, 일부에서는 진단 당시에 원격전이가 진단되기도 하고, 추적관찰 중에 재발을 경험하는 등 공격적 특성을 보인다. 따라서 적극적인 치료와 추적관찰이 필요한 환자를 선별하기 위한 공격적 특성을 갖는 작은 신세포암을 예측할 수 있는 마커가 필요하다. 이에 우리는 투명세포형 신세포암의 공격적 특성을 예측할 수 있는 마커를 탐색하고자 하였다.

2018년 12월부터 2021년 9월까지 T1a 병기의 신세포암으로 수술적 치료를 받은 환자들 중에서 공격적인 특성을 가진 5명의 환자와 공격적 특성을 가지지 않은 5명의 환자로부터 FFPE 샘플을 얻었다. 이 조직들에서 RNA 시퀀싱과 차별 발현 유전자 분석을 수행하였다. 그 후에 2014년 1월부터 12월까지, 우리는 작은 신세포암에 대한 수술을 받은 50명의 환자를 선별하고 PSCA에 대한 면역조직화학 염색을 시행했다. PSCA 발현 정도에 따라 공격적인 작은 신세포암 환자의 비율 차이와 함께, 무재발 생존률을 분석했다. 그리고 신세포암 세포주에서 PSCA 발현을 평가하였으며, 세포주들 중 PSCA 발현이 높은 대표적인 투명세포형 신세포암 세포주인 786-O 세포주를 사용하여 PSCA를 녹다운하였다. 그리고 이에 따른 786-O 세포 증식, 이동성, 침습성 및 콜로니 생성 분석을 시행하였다. PSCA의 기전을 확인하기 위해 mTOR 경로에 존재하는 PI3K, AKT 및 mTOR 단백질의 발현을 비교하였다.

RNA 시퀀싱 결과 총 418개의 차별 발현 유전자가 확인되었으며, Benjamini-Hochberg procedure 후에는 PSCA가 작은 신세포암의 공격적 특성과 관련된 차별 발현 유전자로 확인되었다. 50명의 환자 조직에서 면역조직화학염색을 했을 때, PSCA 양성 그룹에서 PSCA 음성 그룹에 비해 공격적 특성을 갖는 비율이 더 높았으며, 무재발 생존률은 더 낮은 것으로 나타났다. 그리고 786-O 세포에서 PSCA를 녹다운하면 세포 증식의, 이동성, 침습성, 그리고 콜로니 생성 능력이 억제되었다. 또한, PSCA가 녹다운될 때, p-PI3K/PI3K, p-AKT/AKT, 및 p-mTOR/mTOR의 수준이 감소하여, PSCA가 mTOR 경로를 활성화하여 공격성을 획득할 수 있음을 암시하는 것으로 나타났다. 마지막으로 PSCA를 녹다운 했을 때에는 mTOR 차단제인 에버롤리무스에 대한 786-O의 저항성이 증가하는 것으로 나타나, PSCA가

mTOR 차단제 치료의 마커로서의 가능성도 확인하였다.

결론적으로, PSCA는 공격적인 작은 신세포암을 예측할 수 있는 마커인 것으로 보인다. PSCA는 mTOR 경로를 활성화하여 작은 RCC에서 공격적 특성을 갖게 하는 것으로 생각이 되며, mTOR 차단제의 치료 마커의 역할을 할 수 있을 것으로 기대된다.

핵심되는 말: 신세포암, 바이오마커, 전이, 재발